Journal of the Microelectronics & Packaging Society
Vol. 6. No. 2. p.1~12. 1999.

Adhesion Strength Measurements of Cu-based Leadframe/EMC Interface

Ho-Young Lee and Jin Yu

Department of Materials Science and Engineering,
Korea Advanced Institute of Science and Technology, Kusong-dong 373-1,
Yusong-gu, Taejon 305-701, Korea

(Received April 8, 1999;Accepted April 29, 1999)

Abstract : Brown oxide and/or black oxide layers were formed on the surface of Cu-based leadframe by chemical oxidation of leadframe in hot alkaline solutions, and their growth characteristics were studied. Then, to measure the adhesion strength between leadframe and epoxy molding compound (EMC), oxidized leadframe samples were molded with EMC and machined to form sandwiched double-cantilever beam (SDCB) specimens and pull-out specimens, respectively. Results showed that the adhesion strength of un-oxidized leadframe/EMC interface was inherently very poor but could be increased drastically with the nucleation of acicular CuO precipitates on the surface of leadframe. The presence of smooth faceted Cu_2O on the surfaces of leadframe gave close to zero interfacial fracture toughness (G_C) and reasonable pull strength (*PS*). A direct correlation between G_C and *PS* showed that *PS* can be a measure of G_C only in a limited range.

1. INTRODUCTION

In plastic packages, popcorn cracks are frequently generated during the solder reflow process due to the combination of vapor pressure exerting on the delaminated region and thermal stress resulted from the mismatch of the coefficient of thermal expansion (CTE) among package components[1-3].

Since the adhesion strength of Cu-based leadframe/EMC interface is inherently poor, fracture usually follows the leadframe/EMC interface, which is called type-III popcorn crack and a schematic diagram is illustrated in Fig. 1. The procurement of strong Cu-based leadframe/EMC interface is regarded as a key solution to prevent the generation of type-III popcorn crack[1,2,4].

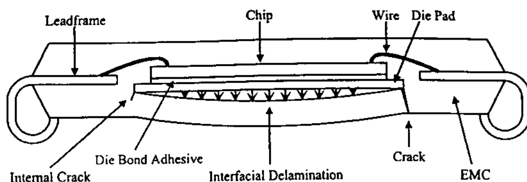

Fig. 1. A schematic diagram of type-III popcorn crack shown on the cross section of package.

In the present work, in order to obtain strong adhesion strength of Cu-based leadframe/EMC interface, two kinds of oxide layers, brown oxide and black oxide layers, were formed on the surface of leadframe by chemical oxidation of copper. After the oxidation, the adh- ion strength of Cu-based leadframe/ MC interface was evaluated in terms of interfacial fracture

toughness, G_C and pull strength, *PS* by using sandwiched double-cantilever beam (SDCB) and pull-out specimens, respectively. Then, measured adhesion parameters, G_C and *PS*, were compared with each other.

2. EXPERIMENTAL PROCEDURE

2.1 Formation of Surface Oxides

A commercial Cu-based leadframe material, EFTEC-64T, with the nominal composition of Cu-0.3Cr-0.25Sn-0.2Zn was provided in the sheet form with the thickness of 0.15 mm. Organic impurities on the surface were removed by ultrasonic cleaning in aceton for 20 minutes and subsequently native oxides were removed by pre-treatment solution (commercial name : Activan #6 offered by Han Yang Chemical Ind. Co. in Korea). After the pre-cleaning process, leadframe samples were immersed in hot alkaline solutions listed in Table I and were maintained less than 20 minutes to form brown oxide and/or black oxide layers on the surface. A schematic diagram of experimental apparatus is shown in Fig. 2. At each stage, oxide layers were analyzed by scanning electron microscope (SEM) and glancing-angle X-ray diffractometry (XRD) with an incident angle of 2°,

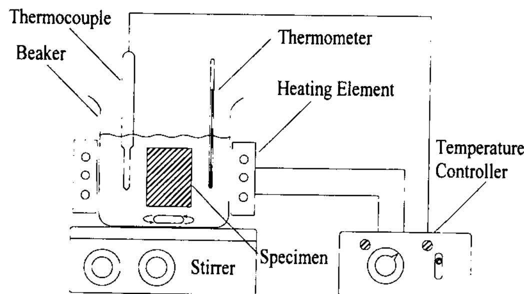

Fig. 2. A schematic diagram of experimental apparatus used to form brown and black oxides.

Table 1. Compositions of solutions and the bath temperature.

Solution(I) (Brown Oxide) [8]	Solution(II)(Black Oxide) [9]
$NaClO_2$(160g/l) NaOH(10g/l) 70℃	$NaClO_2$(37.5g/l) NaOH(50g/l) $Na_3PO_4 \cdot 12H_2O$(100g/l) 95℃

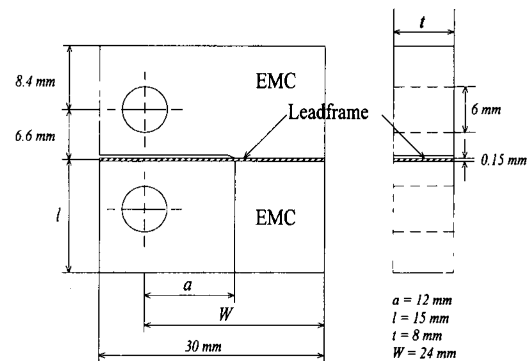

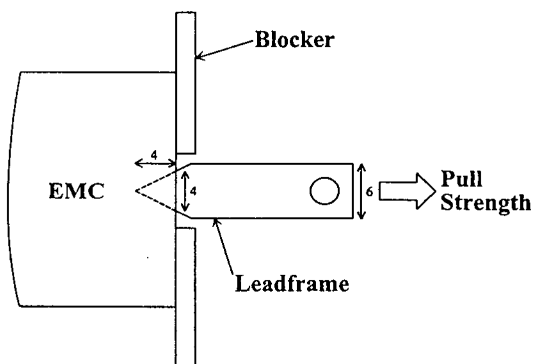

Fig. 3. Schematic diagrams showing the geometry of (a) the sandwiched double-cantilever beam (SDCB) specimen, and (b) the pull-out specimen.

and the thickness of the oxide layer was measured by the galvanostatic reduction method[5-7].

2.2. Preparation of Specimens and Mechanical Tests

After the formation of oxide layers, leadframe samples were compression-molded with EMC under the pressure of 65 Bar for 15 minutes at 175 ℃, and then machined into SDCB specimens which is presented in Fig. 3 (a). Pre-cracks were formed by pasting of correction tape which is used for eliminating miswritten letters. The commercial name of EMC used in this experiment was DMC-20, which corre-ction tape which is use
commercial name of EMC used in this experiment was DMC-20, which was

Table 2. Chemical constituent of EMC.

Component	DMC-20
Filler Content (wt%)	74.5
Type	Fused
Shape	All Flake
Epoxy type	OCN
Hardener type	PN
Catalyst type	Phosphine(triphenyl phosphine)
etc	Strss Modifier(silicone oil)

developed as the encapsulation material for PLCC, VLSI, SOP, FLAT packages by Dong Jin Chemical Co. in Korea. After the machining, post-mold curing (PMC) process was carried out at 175 ℃ for 4 hrs. Since the epoxy is thermosetting polymer, it is necessary to complete the polymerization reaction through PMC process.

Fracture toughness tests were conducted under ambient conditions on the screw-driven Instron model 4206 with a crosshead speed of 0.5 mm/min, and the critical loads at which the onset of fracture process occurred were taken for the interfacial fracture toughness, G_C calculation by following equation[10]:

$$G_C = \frac{12P_C^2a^2}{t^2l^3\overline{E}}\left[3.467+2.315\left(\frac{l}{a}\right)\right]^2 \qquad (1)$$

where, P_C is a critical load, $\overline{E}$ is plane-strain tensile modulus defined as $E/(1-\nu^2)$ (E : Young's modulus, ν : Poisson's ratio), and, a, t, and ℓ are crack length, specimen width, and half specimen-height, respectively. A SDCB specimen can be regarded as a hom-ogeneous specimen when the inserted layer is sufficiently smaller than other specimen geometry[11].

On the other hand, pull-out specimens shown in Fig. 3 (b) were prepared by compression molding of oxidized leadframe samples with EMC. The leadframe part embedded in EMC had a triangular shape to increase the sensitivity of the test, and the same PMC process in SDCB specimens was applied.

Pull-out tests were conducted under ambient conditions on the screw-driven Instron model 4206 with a crosshead speed of 0.5 mm/min, and the critical loads at which the onset of fracture process occurred were taken for the pull strength, PS calculation[12]:

$$PS = \frac{P_C}{A} \qquad (2)$$

where, A is the contact area between

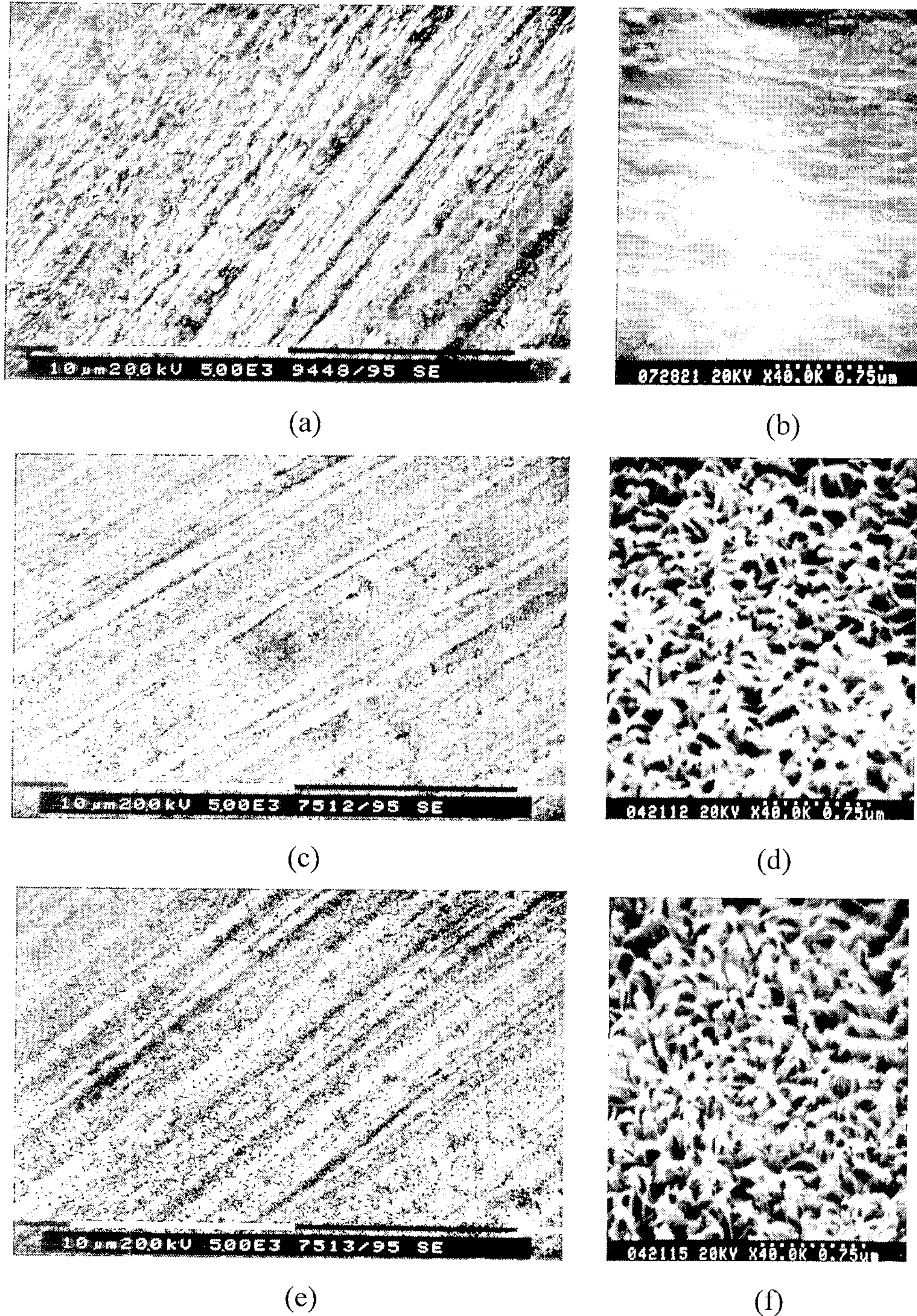

Fig. 4. SEM micrographs taken from the surfaces of leadframes oxidized in the solution (I) : Oxidation times are (a) 0 second, (c) 30 seconds, and (e) 20 minutes. (b), (d), and (f) are magnified images of (a), (c), and (e), respectively.

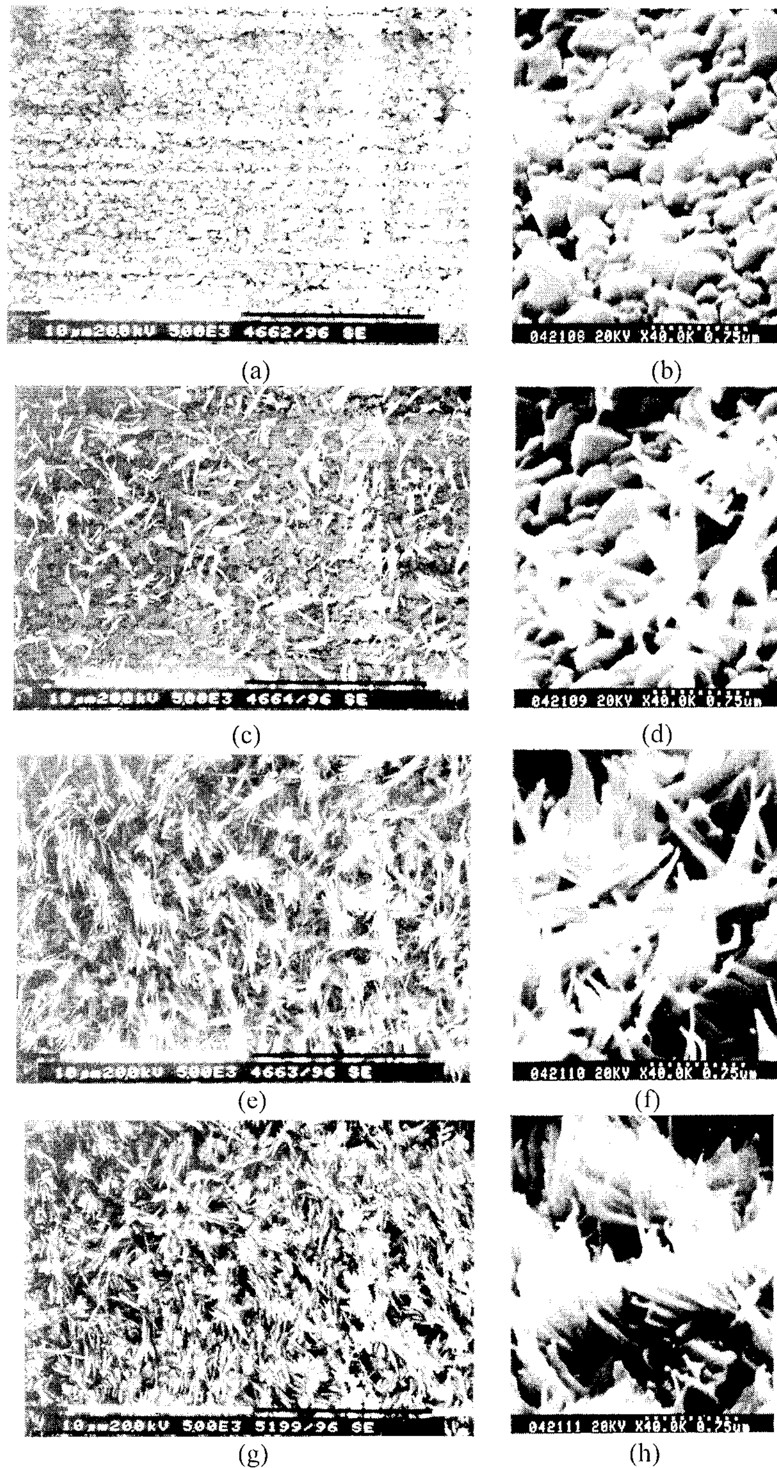

Fig. 5. SEM micrographs taken from the surfaces of leadframes oxidized in the solution (II) : Oxidation times are (a) 30 seconds, (c) 1 minute, (e) 2 minutes, and (g) 20 minutes. (b), (d), (f), and (h) are magnified images of (a), (c), (e), and (g), respectively.

leadframe and EMC, and P_C is a critical load.

Pull-out test has been thought as handy tool for the evaluation of adhesion strength of leadframe/EMC interface[13].

3. RESULTS AND DISCUSSION

3.1. Growth Characteristics of Surface Oxides

After the oxidation of leadframe samples in the alkaline solutions, the surfaces of leadframe samples were examined and analyzed by SEM and glancing-angle XRD, respectively. In addition, the average thickness of oxide layer was measured by galvanostatic reduction method[5-7]. Scanning electron micrographs are presented in Fig. 4 and 5, and corresponding X-ray spectra and thickness of oxide layer are shown in Fig. 6 and 7, respectively.

Figure 4 shows the variation of surface morphology with oxidation time. There can be seen many striations from Fig. 4 (a), which was taken from pre-cleaned leadframe sample. Such striations probably resulted from the cold rolling process to form a sheet shape. The morphologies of the original rolling features were well preserved even until 20 minutes in the case of oxidation in the solution (I). As can be seen from the magnified secondary electron micrographs taken from samples treated in the solution (I), the entire surface is covered with the fine acicular precipitates. XRD and thickness measurement results revealed that those precipitates were CuO crystals and the ave rage thickness of CuO layer increased till ~1.5 minutes obeying following equation;

$$\delta_{CuO} \propto t^{0.86} \ (<1.5) \qquad (3)$$

where, δ_{CuO} is the average thickness of CuO layer (nm) and t is the oxidation time (min). There was no significant change in CuO thickness (~150 nm) after 2 minutes.

On the other hand, the surfaces of leadframe samples oxidized in the solution (II) showed different characteristics. Figure 5 (b) shows pebble-like precipitates with smooth facets. These precipitates were formed on the surface as soon as the leadframe

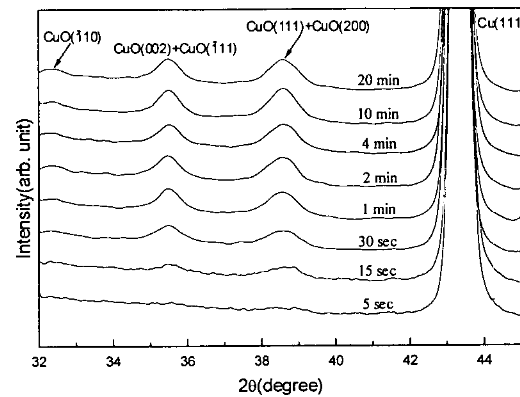

(a)

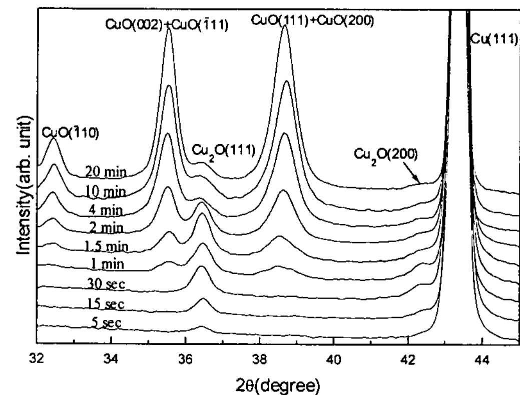

(b)

Fig. 6. Glancing-angle X-ray diffraction patterns out of surfaces of leadframes oxidized in (a) solution (I), and (b) solution (II) at various oxidation times.

sample was dipped into the hot alkaline solution, and coarsened to the average size of 0.2 μm after 0.5~1.0 minute. Through the X-ray analyses, pebble-like precipitates were identified as Cu_2O crystals. The average thickness of Cu_2O layer grew till a minute obeying equation (4) and finally reached ~200 nm.

$$\delta_{Cu_2O} \propto t^{0.89} \ (t<1) \qquad (4)$$

where, δ_{Cu_2O} is the average thickness of Cu_2O layer (nm) and t is the oxidation time (min). After the full growth of Cu_2O crystals, acicular precipitates were nucleated on the Cu_2O layer (see Fig. 5 (c) and (d)) and grew parabolically with the oxidation time.

Newly formed precipitates were afterward confirmed CuO crystals and came to ~1300 nm thickness after 20 minutes. The CuO layer formed on Cu_2O layer was thickened obeying following equation;

$$\delta_{CuO} \propto t^{0.67} \ (2<t<20) \qquad (5)$$

where, δ_{CuO} is the average thickness of CuO layer (nm) and t is the oxidation time (min). Figures 5 (e), (f) and (g), (h) show surface morphologies of leadframe samples oxidized for 2 minutes and 20 minutes, respectively. From these figures, it could be verified that the density of CuO needles is slightly higher in case of the latter than in case of former.

Oxidation of leadframe samples in both solutions (I) and (II) produced acicular CuO crystals on surfaces of leadframes, but the crystal grew up to much larger size in the latter. It will be shown that the adhesion strength between the leadframe and EMC is directly related to the size of CuO needles.

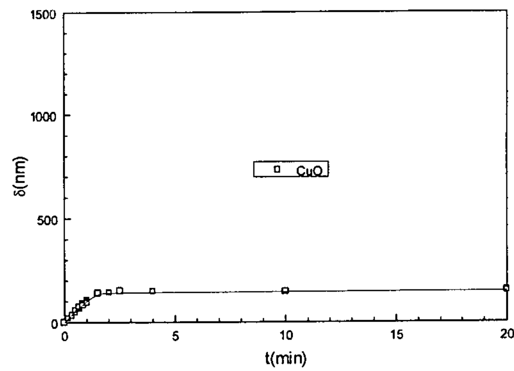

(a)

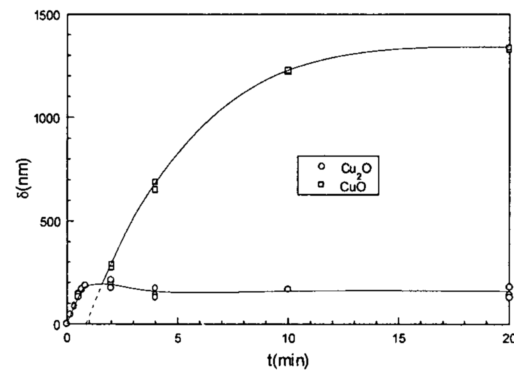

(b)

Fig. 7. Variations of oxide thickness with the oxidation time for specimens treated in (a) solution (I), and (b) solution (II).

3.2. Fracture Toughness Test

Results of the fracture toughness test employing SDCB specimens are given in Fig. 8. In this case, the loading state was close to the pure Mode I loading with a slight Mode II loading. The phase angle, $\hat{\psi}$, which is a measure of the Mode mixity at the crack tip[14] was ~3° for the Cu-based leadframe/EMC system.

$$\psi = \tan^{-1}\left(\frac{K_{II}}{K_I}\right) + \omega(\alpha,\beta) + \varepsilon \ln\left(\frac{\hat{r}}{h}\right) \qquad (6)$$

where, K_I and K_{II} are applied stress intensity factors of Mode I and Mode II, respectively, and $\omega(\alpha,\beta)$, tabulated in the reference [11], is the shift of phase angle due to substrate/ interlayer mismatch of elastic constants. The last

Table 3. Elastic constants of leadframe and EMC.

	Leadframe	EMC
E	1400kg/mm^2	0.25
ν	12500kg/mm^2	0.36

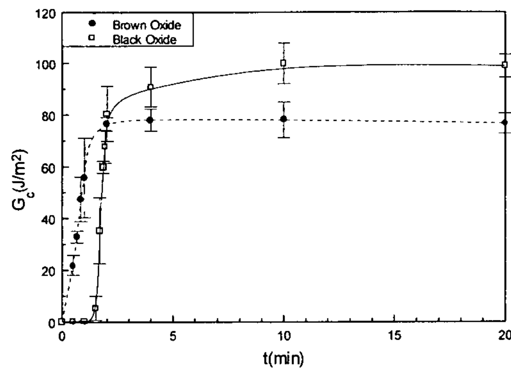

Fig. 8. Fracture toughness of leadframe/ EMC interfaces as a function of the oxidation time. SDCB specimens were loaded under quasi-Mode I loading.

term is Dunders' parameter ε and re-scaling with respect to the ration of characteristic length, $\hat{r}$ to interlayer thickness, h. In this paper, we set the characteristic length $\hat{r}$ for interlayer thickness h (=0.15 mm).

For the leadframe samples oxidized in the solution (I), the fracture toughness of the leadframe/EMC interface, G_C, increased rapidly with the oxidation time up to 2 minutes and reached the saturation value of ~80 J/m^2. The trend in the G_C variation was linearly related to the thickening kinetics of the CuO as shown in Fig. 9. Judging from the facts that there was almost no adhesion between un-oxidized leadframe and EMC, and the linear relationship between G_C and thickness of CuO layer, it might be thought that the adhesion mechanism between brown oxide and EMC is mechanical interlocking.

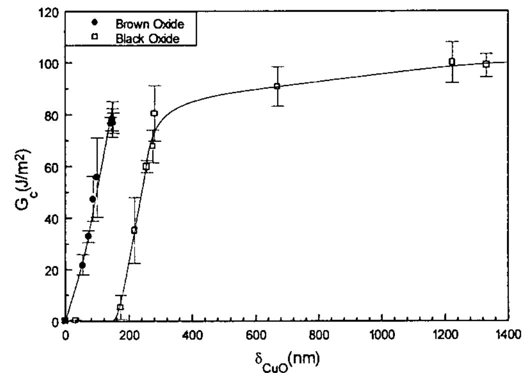

Fig. 9. Correlation between the interfacial fracture toughness and oxide thickness for leadframe samples oxidized in the solution (I), and solution (II).

For the case of oxidation in the solution (II), there was no change in G_C even though the oxidation time elapsed till a minute. There seems to be incubation period in adhesion strength. The incubation period quite coincides with the period when Cu_2O is dominant. On the other hand, as the acicular CuO precipitates occupy the surface of leadframe, the G_C increases abruptly and reached the value of ~80 J/m^2 at 2 minutes. After the 2 minutes of the oxidation time, gradual increase of G_C was observed and reached the saturation value of ~100 J/m^2 around 10 minutes. The entire cover of surface with pebble-like Cu_2O crystals with

smooth facets plays no role in the adhesion, however, once the acicular CuO precipitates appear atop of the Cu_2O layer, there is a great increase in adhesion strength. That implies that adhesion mechanism between black oxide and EMC is mechanical interlocking.

There was a linear correlation between G_C and thickness of CuO ranging from 160 nm to 280 nm. In this range, the thickness of CuO, measured by galvanostatic reduction method, is average thickness so that it cannot reflect the true change of thickness because the CuO layer of oxidation time ranging from 1 to 2 minutes is discontinuous. According to the SEM observation, it is not until the oxidation time is 2 minutes that the CuO layer becomes continuous. Thus, thickness increment in the beginning of CuO formation does not mean the increase in length of CuO needles but the increase in density of CuO needles. From the above results, it is clarified that the adhesion strength between two materials is directly related to the areal coverage of acicular CuO precipitates over the Cu_2O layer in the early stage of CuO formation. At the 2 minutes oxidation time when the CuO layer becomes continuous, the G_C was ~80 J/m^2 and there is no remarkable increase in G_C after that time. This indicates that it is important to become continuous layer and it is relatively less important to become densified layer in aspect of adhesion strength.

At both cases of the oxidation treatments, the maximum toughness values were slightly higher for the oxidation in the solution (II) than in the solution (I) (~100 vs. ~80 J/m^2). These marginal differences in the maximum values can be considered to the needle size difference of acicular CuO crystals and not to the oxide thickness as shown in the previous. Naturally, different needle size of the forefront acicular CuO layer would result in different levels of mechanical interlocking of EMC, in which larger needles turned out to be more effective.

3.3. Pull-out Test

Figure 10 shows the results of pull-out tests for the leadframe samples oxidized in the solution (I). For the un-oxidized leadframe samples (t=0), *PS* was 9 MPa even though G_C was close to zero, and this presumably came from the CTE (α) mismatch between leadframe and EMC. When leadframe samples molded with EMC at the curing temperature T_{cure}, it is reasonable to assume that residual stress between leadframe and EMC is free. However, when the system temperature is changed to room temperature T_{room}, difference in thermal strain (ε) between leadframe and EMC can be expressed as equation (6) under the assumption that α is constant.

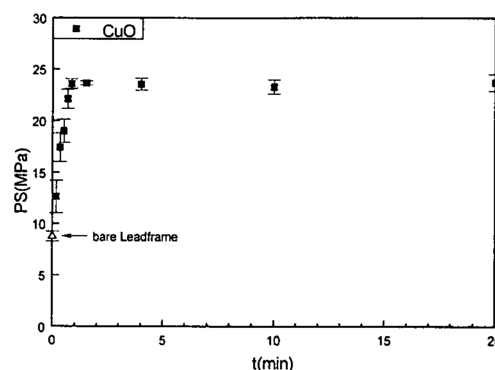

Fig. 10. Pull strength of leadframe/EMC interfaces as a function of the oxidation time of leadframe samples oxidized in the solution (I).

$$\varepsilon_{leadframe} - \varepsilon_{EMC} = (\alpha_{leadframe} - \alpha_{EMC})(T_{room} - T_{cure}) \quad (6)$$

Since $\alpha_{leadframe}$ (17 ppm/°C) < α_{EMC} (α_1 : 16 ppm/°C, α_2 : 67 ppm/°C) and T_{room} < T_{cure}, that therefore $\varepsilon_{leadframe}$ > ε_{EMC}. This means that tensile stress is applied to EMC and at the same time, compressive stress is applied to leadframe. Consequently, EMC contracts the embedded part of the leadframe and induces friction force.

For the oxidized leadframe samples (t > 0), *PS* increased rapidly with increasing oxidation time and reached saturation around 23 MPa after one minute. Even though the overall trend is more or less similar to that of SDCB specimens, it can be noted that *PS* was substantial, and that *PS* saturated slightly earlier than G_C. The differences can be ascribed to friction force and to different characteristics of the two mechanical testing methods used, that is, SDCB specimens have cracks and the stress state of nearly Mode I, but pull-out specimens do not have cracks and the stress state of nearly pure shear. (ModeII). Tensile stress is major driving force for crack propagation in SDCB specimens, and the shear stress is the main driving for crack propagation in pull-out specimens.

Figure 11 shows *PS* of leadframe samples oxidized in the solution (II), and it seems that there are three regions in the plot with regard to the dominant oxide layer on the surface. In a Cu_2O dominant region, there seems to be proportional increase in *PS* with oxidation time. This can be explained thit as the oxidation time elapses, the size of Cu_2O precipitate becomes larger and at the same time their facets develop, so, the surface roughness of leadframe increases, and finally the *PS* increases. The correlation between surface roughness and *PS* with oxidation time is presented in Fig. 12. The increasing trends with oxidation time roughly coincide with each other.

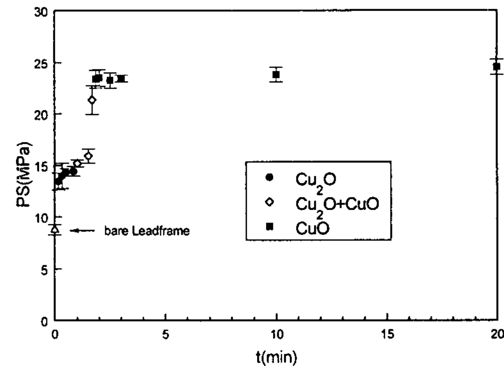

Fig. 11. Pull strength of leadframe/EMC interfaces as a function of the oxidation time of leadframe samples oxidized in the solution (II).

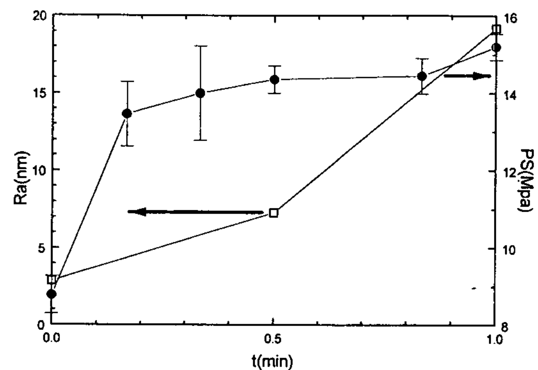

Fig. 12. Surface roughness and pull strength change with the thickness of Cu_2O layer.

In a mixed region which Cu_2O and CuO are intermingled together, *PS* increases rapidly with increasing oxidation time. This might be related to the areal coverage of acicular CuO precipitates over the Cu_2O layer. When the CuO layer became continuous at 2 minutes of the oxidation time,. the *PS* was saturated to ~23 MPa, and it is the point of agreement that the saturation time is the same in compared with the SDCB results. On the other

side, unlike to SDCB results, there is little relationship between the oxidation time and *PS* after 2 minutes. This is because of the almost identical microstructures of oxide after 2 minutes and also of the no change in *PS* with all the densification of CuO layer. The reason why there is little sensitivity in *PS* after 2 minutes is presumably ascribed to that the pull-out test is intrinsically shear test, thus, the variation of density in CuO layer can not exert an influence on the *PS*.

The correlation between fracture toughness (G_C) and the pull strength (*PS*) was presented in Fig. 13. It can be seen that the correlation was very weak except for 15 < *PS* < ~23 MPa. When the adhesion strength was very poor due to weak Cu_2O/EMC interface,

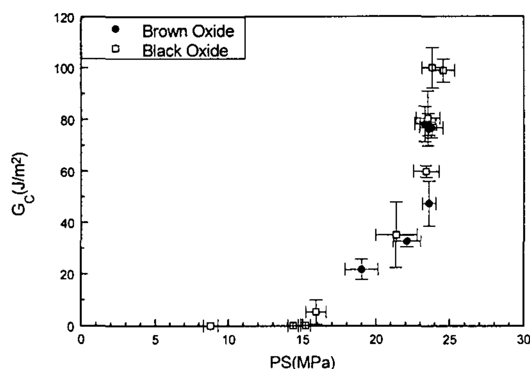

Fig. 13. Correlation between interfacial fracture toughness and pull strength.17

the interface was more resistant to the shear Mode than the normal Mode. When the areal fraction of CuO/EMC interface kept increasing, correlation between G_C and *PS* was good. However, when CuO/EMC interface more or less saturated and CuO layer thickened, only G_C was a sensitive measure because the failure occurred in EMC far away from the CuO/EMC interface in pull-out specimens. The results indicate that one has to be very careful in interpreting *PS* data for presumption of the interfacial fracture toughness. Practically, when the adhesion strength of leadframe/EMC was poor, say 0 < *PS* < 15 MPa, an expectation that G_C would increase proportionally with *PS* can be quite erroneous.

4. CONCLUSIONS

1. In the case of oxidation of Cu-based leadframe in the solution (I), fine acicular CuO crystals nucleated on the surface of leadframe and the CuO layer thickens to ~150 nm within two minutes of the oxidation time. Once a continuous cuo layer covers the entire surface of leadframe, no more oxidation occurs. In a similar manner, G_C of leadframe/EMC interface increases initially with the proportionality with oxidation time and reached a maximum value of ~80 J/m^2 at two minutes. There was no change in G_C with oxidation time after two minutes

2. In the case of oxidation of Cu-based leadframe in the solution (II), pebble-like Cu_2O crystals with smooth facets nucleated initially on the surface of leadframe and the Cu_2O layer thickens to ~200 nm within a minute.

Then, acicular CuO crystals, much larger than those of leadframe samples oxidized in the solution (I), start to nucleate and thicken up to ~1300 nm. G_C of leadframe/EMC interface was close to nil until CuO precipitates start to nucleate after one minute, but increased rapidly to ~80 J/m^2 after two minutes, and finally saturated to ~100 J/m^2.

3. Acicular CuO precipitates contri-uted to the adhesion strength by mechanical interlocking, while smooth-faceted Cu_2O played no role. G_C increased almost linearly until a

continuous layer of CuO crystals formed on the surface of leadframe. Further oxidation just thickened the CuO layer, but increased fracture toughness only marginally.

4. The maximum G_C was slightly higher for the solution (II) (100 vs. 80 J/m^2). The difference can be ascribed to the size of the acicular CuO needles.

5. Since the primary factor affecting G_C of leadframe/EMC interface is the presence of continuous CuO layer at the forefront of interface, the oxidation treatments of two minutes either in solution (I) or solution (II) is good enough to provide superior fracture toughness.

6. *PS* was substantial even for un-oxidized leadframe samples (~9 MPa). This presumably came from the friction force due to the CTE (α) mismatch between leadframe and EMC.

7. In the case of solution (I), *PS* saturated to ~23 MPa after one minute. On the other hand, in the case of solution (II), *PS* saturated to ~23 MPa after four minutes.

8. It seems that *PS* of specimens oxidized in the solution (II) can be divided into three regions with regard to the dominant oxide layer on the surface of leadframe. *PS* increased slightly with the growth of Cu_2O layer, but increased drastically with the growth of CuO layer.

9. Correlations between G_C and *PS* exist only for the limited range of $15 < PS < 23$ MPa. For $PS < 15$ MPa and $G_C > \sim 50$ J/m^2, there was no correlation. An expectation that G_C would increase proportionally with *PS* can be quite erroneous.

REFERENCES

1. C.Lee, W.Hösler, H.Cerva, R.von Criegern and A.Parthasarathi, 48th Electronic Components and Technology Conf., p.1154, (1998)
2. C.Q.Cui, H.L.Tay, T.C.Chai, R.Gopalakrishan and T.B.Lim, 48th Electronic Components and Technology Conf., p.1162, (1998)
3. A.A.O.Tay and T.Y.Lin, 48th Electronic Components and Technology Conf., p.371, (1998)
4. B.H.Moon, H.Y.Yoo and K.Sawada, 48th Electronic Components and Technology Conf., p.1148, (1998)
5. J.R.G.Evans and D.E.Packham, J.Alhesion, Vol. 9, p.267, (1978)
6. V.Ashworth and D.Fairhurst, J. Electrochem. Soc., vol.124, p.506, (1977)
7. H.-H.Strehblow and B.Titze, Electrochemica Acta, vol.55, p.839, (1980)
8. B.J.Love and P.F. Packmam, J.Adhesion, vol.40, p.139, (1993)
9. H.K.Yun, K.Cho, J.H.An and C.E. Park, J. Mater. Sci., vol.27, p.5811 (1992)
10. T.S.Oh, R.M.Cannon and R.O. Ritchie, J. Am. Ceram. Soc., vol.70, p.C-352, (1987)
11. Z.Suo and J.W.Hutchinson, Mater. Sci. and Engng. A, vol.107, p.135, (1989)
12. S.Kim, IEEE Trans. on Components, Hybrids, and Manufacturing Technology, vol.14, p.809, (1991)
13. S.J.Cho, K.W.Paik and Y.G.Kim, IEEE Trans. on Components, Packaging and Manufacturing Technology -Part B, vol.20, p.167, (1997)
14. J.-S. Wang and Z. Suo, Acta Metall. Mater., vol.38, p.1279, (1990)